



Research Paper

Insights into the influence of the cooling profile on the reconstitution times of amorphous lyophilized protein formulations



Karen E. Beech^a, James G. Biddlecombe^b, Christopher F. van der Walle^b, Lee A. Stevens^c, Sean P. Rigby^c, Jonathan C. Burley^a, Stephanie Allen^{a,*}

^a Laboratory of Biophysics and Surface Analysis, School of Pharmacy, University of Nottingham, Nottingham NG7 2RD, UK

^b Formulation Sciences, MedImmune Ltd., Aaron Klug Building, Granta Park, Cambridge CB21 6GH, UK

^c Department of Chemical & Environmental Engineering, University of Nottingham, Nottingham NG7 2RD, UK

ARTICLE INFO

Article history:

Received 30 June 2014

Revised 29 July 2015

Accepted in revised form 31 July 2015

Available online 4 August 2015

Keywords:

Lyophilization

Reconstitution

Mercury intrusion porosimetry

Quench cooling

Annealing

Monoclonal antibody

ABSTRACT

Lyophilized protein formulations must be reconstituted back into solution prior to patient administration and in this regard long reconstitution times are not ideal. The factors that govern reconstitution time remain poorly understood. The aim of this research was to understand the influence of the lyophilization cooling profile (including annealing) on the resulting cake structure and reconstitution time. Three protein formulations (BSA 50 mg/ml, BSA 200 mg/ml and IgG₁ 40 mg/ml, all in 7% w/v sucrose) were investigated after cooling at either 0.5 °C/min, or quench cooling with liquid nitrogen with/without annealing. Significantly longer reconstitution times were observed for the lower protein concentration formulations following quench cool. Porosity measurements found concomitant increases in the surface area of the porous cake structure but a reduction in total pore volume. We propose that slow reconstitution results from either closed pores or small pores impeding the penetration of water into the lyophilized cake.

© 2015 The Authors. Published by Elsevier B.V. This is an open access article under the CC BY license (<http://creativecommons.org/licenses/by/4.0/>).

1. Introduction

To improve the shelf-life and stability of a protein formulation, water can be removed to slow the chemical and physical degradation pathways. The most common method of drying is by lyophilization [1].

Prior to administration the lyophilized product must be reconstituted back into solution, however, for some protein formulations this can be time consuming. For instance, two lyophilized anti-venom products for pit viper snakebites were found to take 40 and >90 min to reconstitute [2]. In addition, higher concentration monoclonal antibody formulations may require 20–40 min for reconstitution [3]. The reconstitution procedure can also differ depending on the product, which can add further complexity to the administration process. For example, after the addition of a diluent, a product may require swirling every five minutes [3], or may be left undisturbed for 30 min to fully reconstitute [4].

A commonly used approach for improving the dissolution time of poorly soluble small drug molecules is by increasing the surface area of the product, for instance by formulating as a solid dispersion [5], or using size reduction techniques [6]. However, recent

research has suggested that surface area is not a predominant factor in reducing the reconstitution times of lyophilized protein formulations. One such study [7], using BSA and a monoclonal antibody as model proteins, found that controlled ice nucleation gave improvements on reconstitution time and proposed this was attributed to the formation of larger pores. However, surface area, which is related to pore size, was not found to be a critical factor for improving reconstitution time in a study investigating multiple parameters such as protein concentration and excipient choice within an Fc-fusion protein formulation [8].

Despite the increasing therapeutic importance of biopharmaceuticals, there have been limited studies on the factors contributing towards long reconstitution time. Therefore, the motivation of the present study was to gain a greater understanding of how two related factors – pore size and surface area – influence the reconstitution time of lyophilized protein formulations. As cooling rate, nucleation temperature, degree of supercooling and heat treatment of a lyophilization cycle can all affect the ice crystal morphology [9] (and therefore the formulation parameters of interest), the present contribution has focussed on the influence of the lyophilization cooling rate on the resulting cake structure. Furthermore, as previous studies have shown either an increase [10], or a decrease [11,12] in reconstitution time of annealed compared to non-annealed samples, the impact of annealing on reconstitution time was also investigated.

* Corresponding author. Tel.: +44 (0) 115 951 5050.

E-mail address: stephanie.allen@nottingham.ac.uk (S. Allen).

2. Materials and methods

2.1. Materials

BSA (molecular weight ~66 kDa), sucrose and histidine buffer salts were all purchased from Sigma–Aldrich. BSA was prepared in a 25 mM histidine buffer solution, pH 6.0, with 7% w/v sucrose to give final concentrations of 50 mg/ml and 200 mg/ml. Monoclonal IgG₁ (molecular weight ~150 kDa), hereafter referred to as 'mAb1', was kindly provided by MedImmune Ltd. at 40 mg/ml in a 25 mM histidine solution, pH 6.0, with 7% sucrose. The three formulations were filtered (0.22 µm) and the protein concentrations were confirmed by UV absorbance at 280 nm (NanoDrop[®], Thermo Fisher Scientific).

2.2. Methods

2.2.1. Lyophilization

The three formulations were lyophilized using a 1 ml fill volume in 13 mm Schott Type I clear tubular 3ml glass injection vials (West Pharmaceutical Services) with Daikyo D777-1 13 mm single vent lyo-stopper (West Pharmaceutical Services). Vials were placed within a custom made stainless steel fence which was used to keep vials in the centre of the freeze dryer. Two freeze dryers were used: a Virtis Advantage Plus two shelf freeze dryer (SP Scientific) for cooling profiles without an annealing step and a Virtis Advantage one shelf freeze dryer (SP Scientific) for cooling profiles with an annealing step. Thermocouples, calibrated before use, were placed into one BSA 50 mg/ml formulation in the centre of the freeze dryer for each cycle. The four cooling profiles can be seen in Table 1, after which the pressure was reduced to 100 mTorr and the temperature was raised to –20 °C and held for 41.5 h to allow primary drying. The shelf temperature was then ramped at 0.1 °C/min to 20 °C for secondary drying and held at this temperature for 12 h at 200 mTorr.

2.2.2. Karl Fisher moisture determination

After each lyophilization cycle, three vials of each BSA formulation were removed. The residual water content was determined by injecting 2 ml of methanol into sealed vials which was then mixed in a vortex for 15 min to extract the moisture and analysed by a Mettler Toledo C30 Coulometric Karl Fischer Titrator. The mAb1 formulation was not used for this analysis due to the limited number of samples lyophilized.

2.2.3. Scanning Electron Microscopy (SEM)

Samples were prepared for analysis using SEM stubs in a dry argon box. To alleviate compression of the cake during preparation, a sharp scalpel was used to cut the lyophilized material to expose an internal cross section. A Leica EM SCD005 sputter coater (Leica Microsystems) was used to coat samples in gold for 120 s at

26 mAmps. A JEOL JSM 6060LV SEM (JEOL Ltd.) was used with an accelerating voltage of 16 kV.

2.2.4. Brunauer, Emmett & Teller (BET) specific surface area measurements

BET adsorption theory [13] was used to calculate the specific surface area of the lyophilized formulations. Nitrogen isotherms were acquired using an Automated Surface Area Porosity Analyser (ASAP2420, Micromeritics Instrument Corporation) at –195.8 °C using a relative pressure range of 0.01–0.99. Prior to analysis samples (weight 100–150 mg) were gently broken using a spatula and were then degassed under vacuum for 3 h at ambient temperature. Helium gas was used to calculate warm (ambient) and cold free space. BET specific surface area (SSA) was calculated using the adsorption range of 0.1–0.4 relative pressure providing positive BET constants.

2.2.5. Mercury Intrusion Porosimetry (MIP)

Mercury intrusion porosimetry was performed using an AutoPore IV Mercury Porosimeter (Micromeritics Instrument Corporation) on samples used for BET analysis with measurements taken between 1 and 3600 psi. A contact angle of 130° was used with mercury density adjusted according to room temperature. Samples were weighed after MIP and observed for signs of compression. Again, due to the limited number of mAb1 samples, only the BSA formulations were used for this analysis. Bulk density was calculated using a pressure of 0.51 psi.

2.2.6. Reconstitution time

The volume of water required for reconstitution was calculated based on the amount of water removed from each formulation (i.e. total weight less the amount of solids). This value was then rounded to the nearest 0.1 ml, based on the graduation of syringes found in a hospital setting. For BSA 50 mg/ml and mAb1 40 mg/ml formulations, 0.9 ml of water was used for reconstitution and for BSA 200 mg/ml 0.8 ml of water was used. Prior to reconstitution, the samples requiring different reconstitution volumes were separated and the formulation labels blinded to randomize the cooling profiles and maintain a level of objectivity. Samples were then reconstituted using a syringe with the water low aimed at the inside wall of the vial. The vial was then swirled for approximately five seconds to ensure the sides and bottom of the lyophilized cake were wetted. The vial was then left upright on a counter without further agitation until fully dissolved. This static procedure was chosen in order to minimize variability in the reconstitution time determination. The reconstitution time was defined as the time needed to dissolve all visible solids in the vial from the point of water injection. Six vials of each formulation were reconstituted. Statistical analyses were performed using a one-way analysis of variance with Bonferroni correction.

Table 1

A description of the protocol followed for each lyophilization cooling profile.

| | Cooling profile |
|--------------------------|---|
| 0.5 °C/min | Samples were cooled at 0.5 °C/min to –40 °C and held for two hours. |
| 0.5 °C/min + annealed | Samples were cooled at 0.5 °C/min to –40 °C and held for two hours. The temperature was then ramped over 30 min to –5 °C and held for four hours after which the shelf temperature was lowered over 30 min to –40 °C and held for a further 30 min |
| Quench cooled | Samples were immersed for approximately 2 min in liquid nitrogen and then placed onto the freeze dryer shelf, which was pre-cooled to –40 °C. This shelf temperature was then maintained for two hours |
| Quench cooled + annealed | Samples were immersed for approximately 2 min in liquid nitrogen and then placed onto the freeze dryer shelf, which was pre-cooled to –40 °C. This shelf temperature was then maintained for two hours after which it was ramped over 30 min to –5 °C and held for four hours before lowering it over 30 min to –40 °C and holding for a further 30 min |

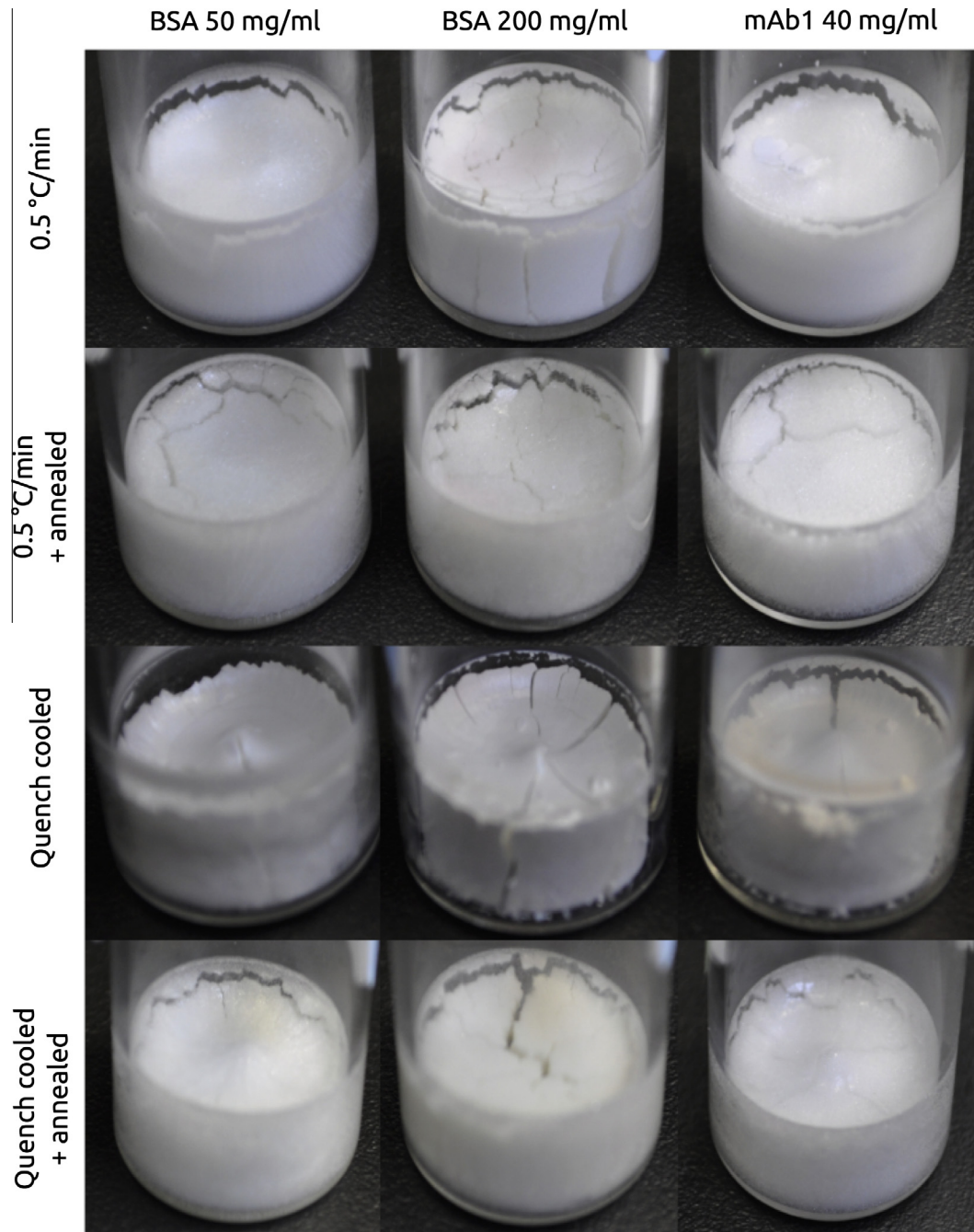


Fig. 1. The appearance of the different protein formulations after lyophilization.

3. Results

3.1. Lyophilized cake appearance

After lyophilization, representative cakes were evaluated and found to be amorphous. On visual inspection, small scale uniform cake shrinkage and cracking were observed for all samples and, to a greater extent, with quench cooled only samples in which the cakes were no longer in contact with the sides of the vial (Fig. 1). This was likely due to a high amount of unfrozen amorphous water remaining in the formulation prior to desorption during secondary drying. Macro-collapse, in which there is significant shrinkage and loss of structural integrity of the cake, was not evident in the samples.

3.2. Reconstitution time

The reconstitution times of the three lyophilized formulations are shown in Fig. 2. The change in protein secondary structure was also evaluated by IR spectroscopy second derivative analysis (data not shown). For all formulations at least 96% conservation in secondary structure was found in the reconstituted formulations, when compared to the solution state, prior to lyophilization. The reconstitution times of BSA 50 mg/ml and mAb1 formulations were found to be significantly longer in samples lyophilized by quench cooling. Increasing the BSA concentration from 50 mg/ml to 200 mg/ml led to longer reconstitution times of up to approximately 40 min, although no statistically significant differences were observed between the different cooling profiles.

3.3. Pore appearance by SEM

Two distinct pore geometries were created by the different cooling profiles: interconnected spherical shaped pores from 0.5 °C/min and annealing profiles, and cylindrical pores after quench cooling without an annealing step (Fig. 3). The spherical shaped pores likely reflect ice crystal growth through a global supercooling process, where ice can form stable hexagonal dendrites [14,15]. During annealing, ice crystals can grow through re-crystallization processes such as Ostwald ripening where larger ice crystals grow at the expense of smaller crystals, the increased molecular mobility of which is provided by the higher temperatures during annealing [12]. The lamellar structure observed for quench cooled samples is the likely result of ice growth through directional solidification where, due to the fast freezing rate, spherulites (ice spears) form without side branches [16]. The change from cylindrical to spherical shaped pores during annealing of fast cooled samples has previously been reported [12].

3.4. Surface area and moisture measurements

The BET specific surface area (SSA) and residual moisture contents (BSA formulations only) for the lyophilized samples can be seen in Fig. 4. Quench cooled samples were found to have the largest BET SSA at approximately 3 m²/g. The increased surface area of samples prepared by quench cooling compared to those frozen slowly is consistent with other literature [17]. Samples that were lyophilized with an annealing step in the cooling profile were

found to have the lowest BET SSA, which is consistent with SEM images that showed the appearance of larger pores in annealed samples. The residual moisture contents, measured by Karl Fisher titration, were all found to be less than 1%, which is a suitable level for a lyophilized protein formulation [18]. The residual moisture content for the BSA 50 mg/ml formulation was found to be lower after quench cooling compared to the other cooling profiles. This is likely due to the larger SSA which allows faster water desorption rates resulting in less residual moisture within the lyophilized cake [19].

3.5. Porosimetry measurements

The pressure which allows mercury, a non-wetting probe, to intrude into a porous sample can be used to determine the inner pore aperture size through the relationship described by the Washburn equation [20]. For each BSA formulation and cooling profile, three samples were analysed (Fig. 5). The pore size distributions of these three samples appear in good agreement with each other suggesting that the cake structure is reproducible within the batch, depending on the initial formulation and processing parameters.

One broad pore size distribution was observed between 10 and 50 µm for BSA 50 mg/ml lyophilized at a 0.5 °C/min cooling rate. With the addition of an annealing step, a trimodal pore distribution was observed after both 0.5 °C/min and quench cooling rates. A bimodal size distribution was observed with BSA 50 mg/ml after quench cooling: the first between 1 and 8 µm and the second

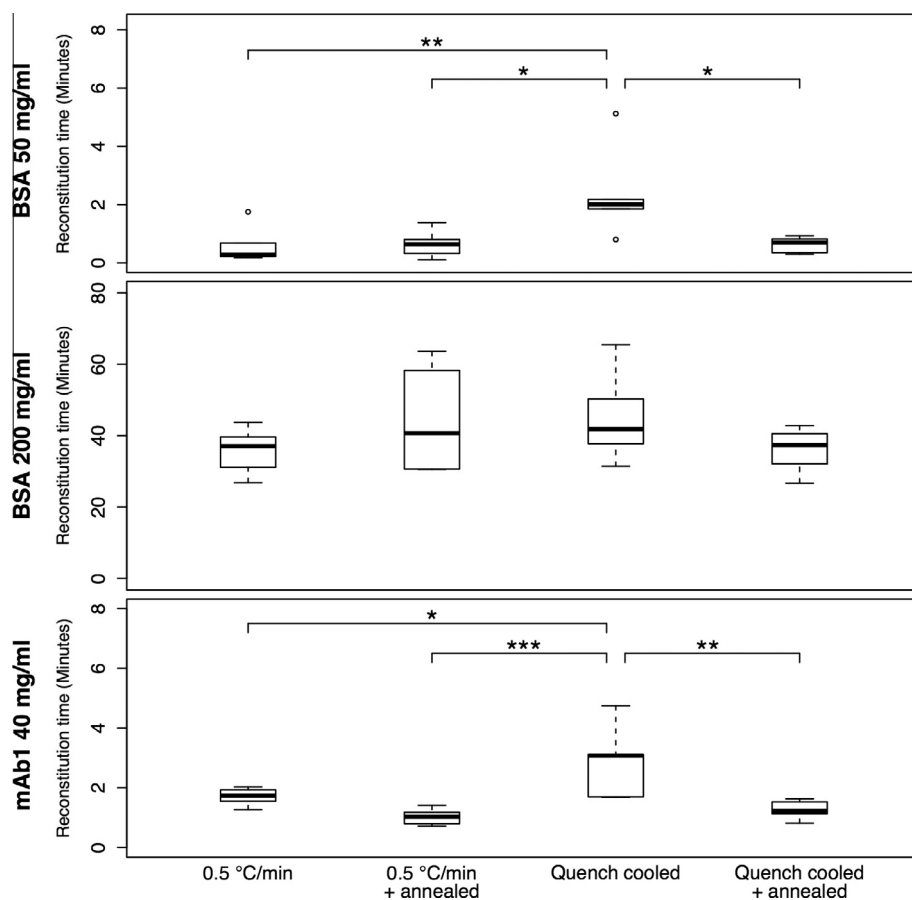


Fig. 2. The reconstitution times of the three lyophilized formulations using four different cooling profiles, ($n=6$). Statistically significant differences are denoted by * ($p < 0.05$), ** ($p < 0.01$) and *** ($p < 0.001$). Please note the difference in y-axis scale. Each box plot represents the interquartile range with the median as the thick horizontal line. Dashed lines show the minimum and maximum reconstitution times. Outliers, defined as being greater than 1.5 times the distance from the lower and upper quartiles are shown as circles.

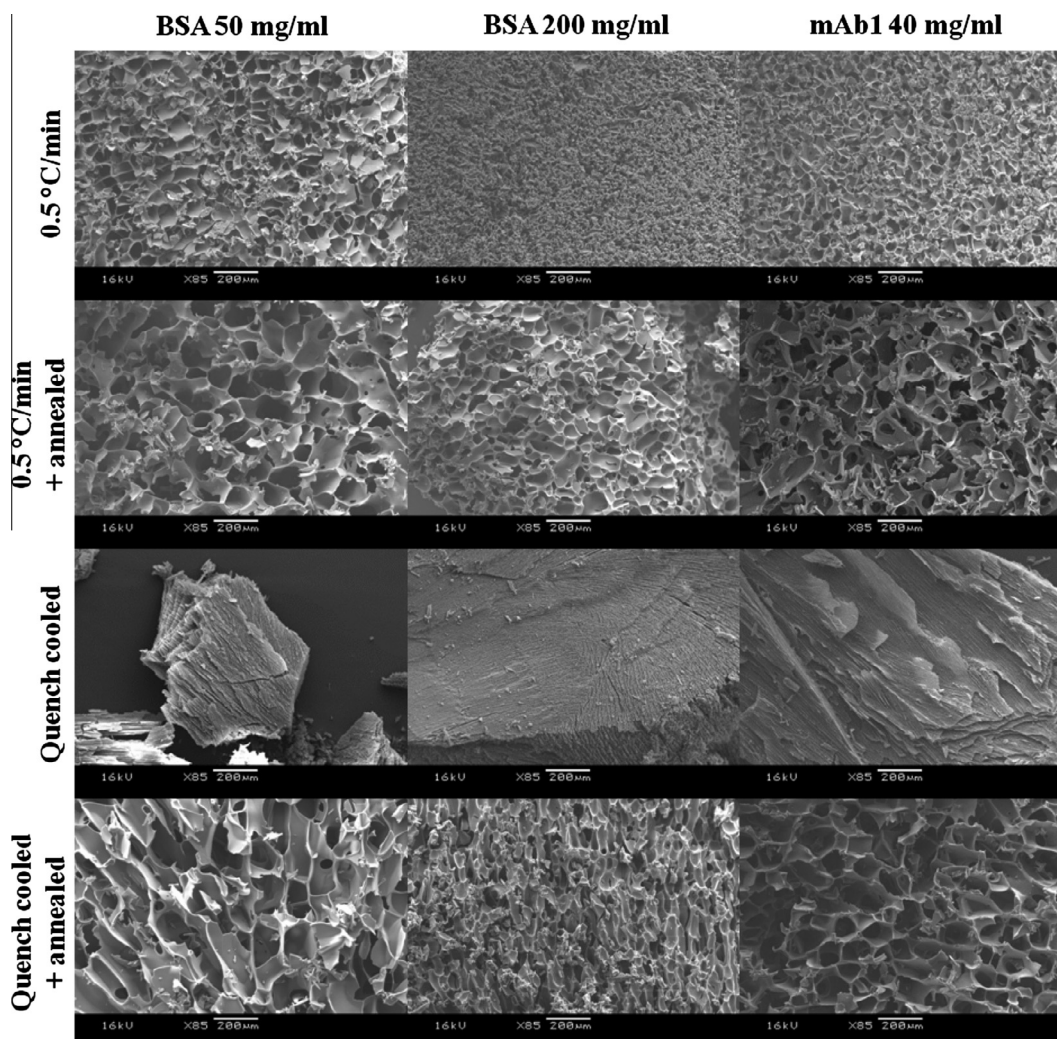


Fig. 3. The appearance (by SEM) of the different protein formulations after lyophilization.

between 8 and 50 μm (with the majority of pores between 10 and 20 μm). Only one pore size distribution can be distinguished for the 200 mg/ml BSA formulation where, after 0.5 °C/min and quench cooled profiles, pore sizes appear less than 5 μm in diameter. After annealing the pore sizes increase to approximately 10–20 μm .

In Figs. 6 and 7 the bulk density and total pore volume, derived from MIP experiments, have been shown, respectively. The bulk density of samples was measured by applying a pressure that allowed mercury to surround the sample without penetrating into the pores (0.51 psi). The resulting sample volume therefore includes both solid material and pore spaces. The total pore volume of the samples was determined using the volume of mercury intruded into the sample (up to a pressure of 3600 psi). Although bulk density and total pore volume have been shown separately, their multiplication can be used to describe the porosity of the sample. No significant differences were observed in bulk density between the different cooling profiles of the lyophilized BSA 200 mg/ml formulation. For the BSA 50 mg/ml cakes, a significantly higher bulk density and lower total pore volume were observed after quench cooling compared to the annealed samples.

4. Discussion

The key result from this study is that significantly longer reconstitution times were observed for the quench cooled BSA 50 mg/ml

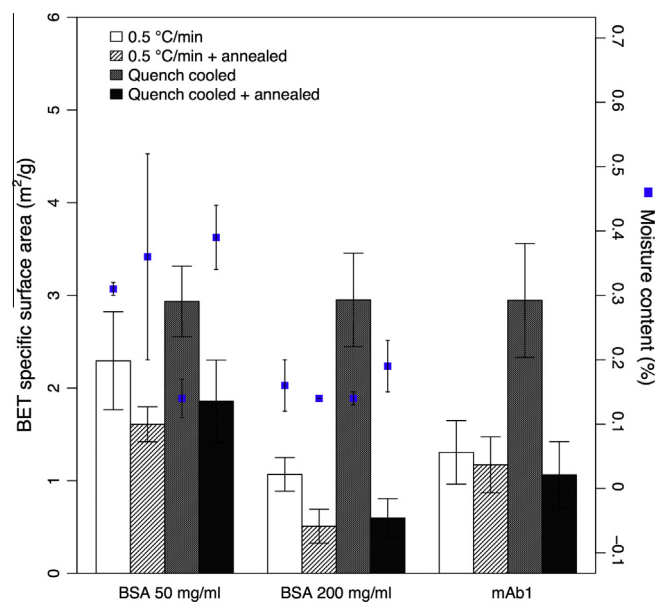


Fig. 4. The BET specific surface area of lyophilized formulations and the corresponding residual moisture contents (shown for BSA formulations only) ($n = 3$, mean \pm s.d.).

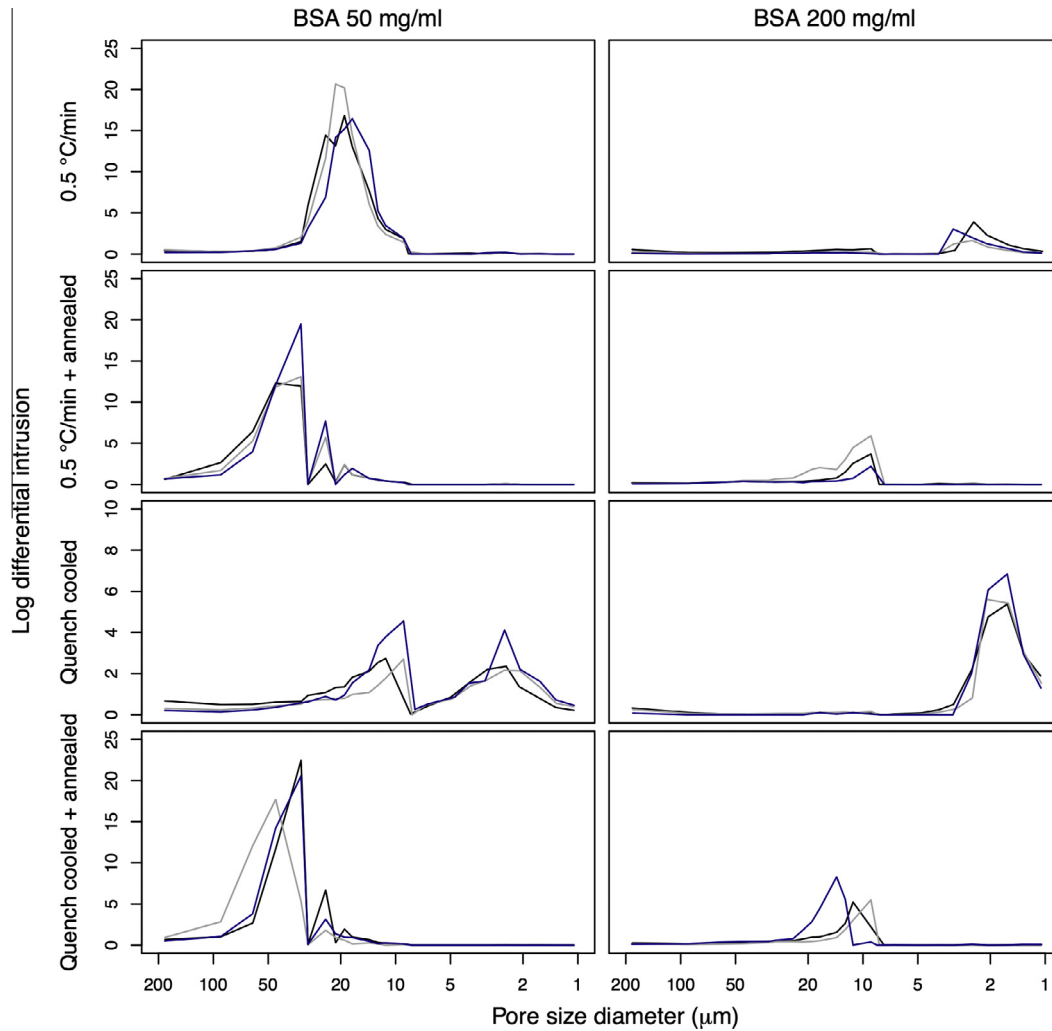


Fig. 5. The log differential intrusion of mercury into the two BSA formulations. Three vials of each formulation were analysed and are shown separately. Please note the different scale for quench cooled samples.

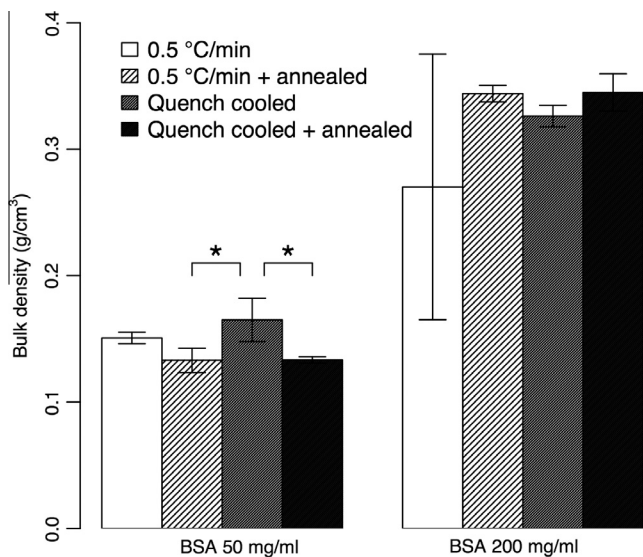


Fig. 6. The bulk density of lyophilized BSA formulations ($n = 3$, mean \pm s.d.). Statistically significant differences are denoted by $^*(p < 0.05)$.

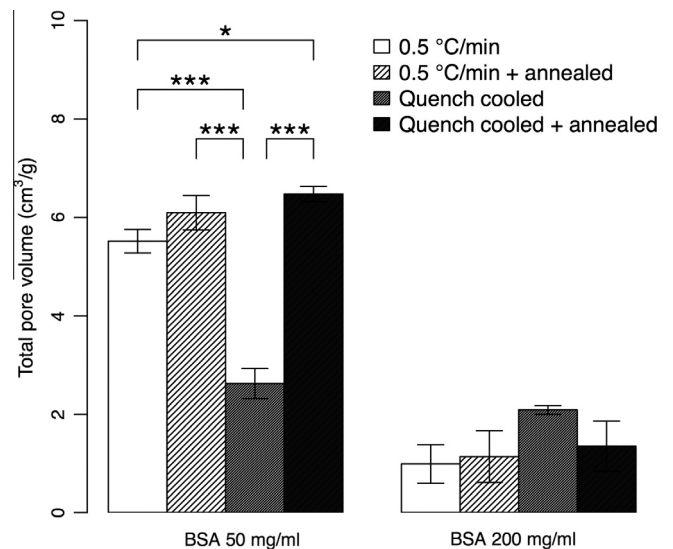


Fig. 7. The total pore volume of BSA formulations ($n = 3$, mean \pm s.d.). Statistically significant differences are denoted by $^*(p < 0.05)$ and $^{***}(p < 0.001)$.

and mAb1 formulations, despite having the greater surface area. These results are consistent with other recent research [7,8,21] and we also conclude that surface area was not a predominant factor in determining lyophilized cake reconstitution time.

For the BSA 200 mg/ml formulation, altering the lyophilization cooling profile was not found to significantly affect the reconstitution time of the lyophilized cakes. The observed increase in reconstitution time compared to BSA 50 mg/ml and mAb1 formulations, may be explained by concentration effects altering the solution viscosity. At high concentrations, self-association of the protein can lead to large increases in its viscosity [22], thus retarding diffusion-controlled reconstitution. As vials were left undisturbed after initial wetting in this study, the reconstitution process may also have been further prolonged by allowing the establishment of high concentration and high viscosity regions within the cake. Although viscosity and protein self-association measurements were outside the scope of this work, which focussed on surface area and porosimetry measurements, it is acknowledged that these factors would need to be taken into account in more detailed models of fluid flow and diffusion processes underpinning the reconstitution processes.

For the lower concentration protein formulations investigated in this study, two important structural features are believed to have led to the reconstitution times observed, namely the presence of closed pores and the size of pores. In other studies [23,24], the openness and connectivity of pores has been found to be important for decreasing vapour transit resistance during lyophilization. Conversely, a more open network of pores could also allow better penetration of the diluent into the lyophilized cake.

The loss of total pore volume with quench cooled BSA 50 mg/ml cakes may be partially caused by closed pores in the lyophilized material. The higher bulk density in these samples compared to the other cooling profiles also suggests that there is some collapse of the cake structure [25], which is consistent with the greater degree of volumetric shrinkage observed with the quench cooled samples. In addition to volumetric shrinkage, high amorphous water content during secondary drying may lead to changes in the microstructure of the cake which could alter the reconstitution process, although this has yet to be corroborated in the literature. The poor intrusion of mercury into samples with closed pores may also correspond with poor penetration of water into the cake, thus prolonging reconstitution times.

Two pore size distributions were observed with quench cooled BSA 50 mg/ml samples. From the SEM images (Fig. 3), the smaller pore size appears consistent with the width of the cylindrical pores observed. It is possible that the size distribution of larger pores may have resulted from breakage of the pore walls, leading to wider apertures. After annealing of the BSA 50 mg/ml sample, a trimodal pore size distribution was evident after 0.5 °C/min and quench cooling rates. It is possible that the different size distributions result from ice crystals, which vary in size between the bottom and top of the vial [26]. Ostwald ripening, which can occur during annealing, could also lead to an increase in the mean pore size and changes in the pore size distribution [12]. However, it is likely that these mechanisms would lead to a continuous, rather than a trimodal, distribution of pore sizes. Discrete pore size distributions have not previously been reported within this research field and suggest that the annealing process during lyophilization may be more complex than previously thought.

Rather than the number of pore size distributions, it is likely that the size of the pores (and the volume that they occupy in the sample), would affect the reconstitution time. Both Darcy's Law, which describes the permeability of a fluid through a porous material [27], and the Hagen–Poiseuille equation, which relates flow rate through a cylinder, (Eq. (1)), describe permeability/flow

rate as being directly proportional to the pore size in a power-law relationship:

$$Q = \frac{\pi R^4 \Delta P}{8\eta L} \quad (1)$$

where Q is the volumetric flow rate, R is the radius of the cylinder that has a length of L , ΔP is the change in pressure across the cylinder and η is the viscosity of the medium. The relationship between flow rate and pore size described by the Hagen–Poiseuille equation can have important consequences when comparing samples with different pore diameters of, for example: 2, 20 and 50 μm (which are similar to those observed in Fig. 5 for BSA 50 mg/ml quench cooled, cooled at 0.5 °C/min and annealed samples, respectively). Through simple calculation, a 10,000-fold increase in flow rate is expected if pore diameter is increased from 2 to 20 μm . However, only a 40-fold increase occurs between pores that are 20 and 50 μm in diameter. The longer reconstitution times that were observed with the BSA 50 mg/ml quench cooled samples may be explained by this theory, as approximately half of the pore volume was associated with pores that were approximately 2 μm in diameter. It is interesting to consider that if a power-law relationship does exist between pore size and reconstitution time, then there may also be a critical pore size below which reconstitution time will be prolonged by slow water penetration into the lyophilized cake.

5. Conclusions

The lyophilization cooling rate, but not annealing, was found to affect the reconstitution time of two lyophilized protein formulations. However, the significance of this appears also to be dependent on the protein concentration. This work is consistent with other recent studies and has found that an increase in specific surface area of the formulation did not decrease reconstitution time. Rather, the shorter reconstitution times for the BSA 50 mg/ml and mAb1 formulations were likely due to the more open network of larger spherical pores (as observed in SEM images), compared to quench cooled cakes with narrower cylindrical pores. Further consideration should be given to the power-law relationships describing fluid flow through porous networks, and a possible “cut-off” in pore size below which the increase in reconstitution time becomes impractical for lyophilized formulations.

Acknowledgements

This study was supported by the Targeted Therapeutics Centre for Doctoral Training (University of Nottingham) which is jointly funded by AstraZeneca and the Engineering and Physical Sciences Research Council (Grant EP/D501849/1).

References

- [1] S.D. Allison, T.W. Randolph, M.C. Manning, K. Middleton, A. Davis, J.F. Carpenter, Effects of drying methods and additives on structure and function of actin: mechanisms of dehydration-induced damage and its inhibition, *Arch. Biochem. Biophys.* 358 (1) (1998) 171–181.
- [2] R.E. Hill, G.M. Bogdan, R.C. Dart, Time to reconstitution: purified Fab antivenom vs. unpurified IgG antivenom, *Toxicon* 39 (5) (2001) 729–731.
- [3] How to Prepare & Administer XOLAIR, Genentech, Inc. and Novartis Pharmaceuticals Corporation, 2014, Available from: <<http://www.xolair.com/hcp/how-to-prepare-and-administer-xolair.html#accordionTab2>>, (accessed 25.04.14).
- [4] Highlights of Prescribing Information, UCB, Inc.; 2013, Available from: <www.cimzia.com/assets/pdf/Prescribing_Information.pdf>, (accessed 18.01.15).
- [5] C. Leuner, J. Dressman, Improving drug solubility for oral delivery using solid dispersions, *Eur. J. Pharm. Biopharm.* 50 (1) (2000) 47–60.
- [6] E. Merisko-Liversidge, G.C. Liversidge, E.R. Cooper, Nanosizing: a formulation approach for poorly-water-soluble compounds, *Eur. J. Pharm. Sci.* 18 (2) (2003) 113–120.

- [7] R. Geidobler, I. Konrad, G. Winter, Can controlled ice nucleation improve freeze-drying of highly-concentrated protein formulations?, *J. Pharm. Sci.* 102 (11) (2013) 3915–3919.
- [8] W. Cao, S. Krishnan, M.S. Ricci, L.Y. Shih, D. Liu, J.H. Gu, et al., Rational design of lyophilized high concentration protein formulations—mitigating the challenge of slow reconstitution with multidisciplinary strategies, *Eur. J. Pharm. Biopharm.* 85 (2) (2013) 287–293.
- [9] B. Chang, S. Patro, Freeze-drying process development for protein pharmaceuticals, in: H. Costantino, M. Pikal (Eds.), *Lyophilization of Biopharmaceuticals*, American Association of Pharmaceutical Scientists, Arlington, VA, 2004, pp. 113–138.
- [10] S. Webb, J. Cleland, J. Carpenter, T. Randolph, Effects of annealing lyophilized and spray-lyophilized formulations of recombinant human interferon-gamma, *J. Pharm. Sci.* 92 (4) (2003) 715–729.
- [11] J. Blue, H. Yoder, Successful lyophilization development of protein therapeutics, *Am. Pharm. Rev.* 12 (2009) 90–96.
- [12] J. Searles, J. Carpenter, T. Randolph, Annealing to optimize the primary drying rate, reduce freezing-induced drying rate heterogeneity, and determine T_g' in pharmaceutical lyophilization, *J. Pharm. Sci.* 90 (7) (2001) 872–887.
- [13] S. Brunauer, P. Emmett, E. Teller, Adsorption of gases in multimolecular layers, *J. Am. Chem. Soc.* 60 (2) (1938) 309–319.
- [14] J.C. Kasper, W. Friess, The freezing step in lyophilization: physico-chemical fundamentals, freezing methods and consequences on process performance and quality attributes of biopharmaceuticals, *Eur. J. Pharm. Biopharm.* 78 (2) (2011) 248–263.
- [15] T.A. Felix Franks, *Essential physics of low temperature and freezing, Freeze-drying of Pharmaceuticals and Biopharmaceuticals: Principles and Practice*, The Royal Society of Chemistry, Cambridge, UK, 2007, pp. 28–53.
- [16] G. Petzold, J.M. Aguilera, Ice morphology: fundamentals and technological applications in foods, *Food Biophys.* 4 (4) (2009) 378–396.
- [17] J. Sarciaux, S. Mansour, M. Hageman, S. Nail, Effects of buffer composition and processing conditions on aggregation of bovine IgG during freeze-drying, *J. Pharm. Sci.* 88 (12) (1999) 1354–1361.
- [18] W. Wang, Lyophilization and development of solid protein pharmaceuticals, *Int. J. Pharm.* 203 (1–2) (2000) 1–60.
- [19] M. Pikal, S. Shah, M. Roy, R. Putman, The secondary drying stage of freeze-drying – drying kinetics as a function of temperature and chamber pressure, *Int. J. Pharm.* 60 (3) (1990) 203–217.
- [20] E.W. Washburn, The dynamics of capillary flow, *Phys. Rev.* 17 (1921) 273–283.
- [21] D. Awotwe-Otoo, C. Agarabi, E.K. Read, S. Lute, K.A. Brorson, M.A. Khan, et al., Impact of controlled ice nucleation on process performance and quality attributes of a lyophilized monoclonal antibody, *Int. J. Pharm.* 450 (1–2) (2013) 70–78.
- [22] S.J. Shire, Z. Shahrokh, J. Liu, Challenges in the development of high protein concentration formulations, *J. Pharm. Sci.* 93 (6) (2004) 1390–1402.
- [23] D. Overcashier, T. Patapoff, C. Hsu, Lyophilization of protein formulations in vials: investigation of the relationship between resistance to vapor flow during primary drying and small-scale product collapse, *J. Pharm. Sci.* 88 (7) (1999) 688–695.
- [24] R.E. Johnson, M.E. Oldroyd, S.S. Ahmed, H. Gieseler, L.M. Lewis, Use of manometric temperature measurements (MTM) to characterize the freeze-drying behavior of amorphous protein formulations, *J. Pharm. Sci.* 99 (6) (2010) 2863–2873.
- [25] M.K. Krokida, V.T. Karathanos, Z.B. Maroulis, Effect of freeze-drying conditions on shrinkage and porosity of dehydrated agricultural products, *J. Food Eng.* 35 (4) (1998) 369–380.
- [26] A. Hottot, S. Vessot, J. Andrieu, Freeze drying of pharmaceuticals in vials: Influence of freezing protocol and sample configuration on ice morphology and freeze-dried cake texture, *Chem. Eng. Process.* 46 (7) (2007) 666–674.
- [27] G.O. Brown, Henry Darcy and the making of a law, *Water Resour. Res.* 38 (7) (2002) 11–11–12.